



# Simultaneous destruction of Nickel (II)-EDTA with TiO<sub>2</sub>/Ti film anode and electrodeposition of nickel ions on the cathode

Xu Zhao, Libao Guo, Chengzhi Hu, Huijuan Liu, Jiahui Qu \*

State Key Laboratory of Environmental Aquatic Chemistry, Research Center for Eco-Environmental Sciences, Chinese Academy of Sciences, Beijing 100085, PR China

## ARTICLE INFO

### Article history:

Received 2 May 2013

Received in revised form 7 July 2013

Accepted 15 July 2013

Available online 24 July 2013

### Keywords:

Heavy metal

Ni-EDTA

Photoelectrocatalysis

Electrodeposition

## ABSTRACT

Ethylenediaminetetraacetic acid (EDTA) forms stable complexes with toxic metals such as nickel. A combined photocatalytic-electrochemical system using TiO<sub>2</sub>/Ti plate as anode and stainless steel as cathode achieves the simultaneous decomplexation of Ni-EDTA and recovery of nickel. Ni-EDTA was efficiently destroyed in photoelectrocatalytic process in comparison with individual photocatalytic and electro-oxidation process. At 60 min, removal efficiencies of Ni-EDTA were 75%, 12%, and 5%, respectively. At 180 min, the removal efficiency of Ni-EDTA in the photocatalysis and electrolysis processes is only 21% and 18%, respectively. By contrast, nearly 90% Ni-EDTA is removed in the photoelectrocatalytic process. The recovery percentage of nickel was determined to be 45%, 21%, and 5% in the photoelectrocatalysis, electrolysis, and photocatalysis process, respectively. The deposition of nickel ions at the cathode was confirmed by scanning electron microscopy analysis and the nickel species were identified via X-ray photoelectron spectra as nickel with zero value. The removal of Ni-EDTA and recovery of nickel ions increased with the current density and favored at acid conditions. Intermediates detected using a capillary electrophoresis and a high performance liquid chromatography includes Ni-NTA, glycine, maleic acid, glycolic acid, formic acid, acetic acid, oxalic acid, and oxamic acid were identified. The decomplexation pathway of Ni-EDTA was proposed.

© 2013 Elsevier B.V. All rights reserved.

## 1. Introduction

Ethylenediaminetetraacetic acid (EDTA) is a common chelating agent used in many different industrial applications for sequestration of metal ions. It has been frequently detected in the environment [1]. And, EDTA can make it difficult to remove heavy metals in wastewaters by conventional chemical precipitation processes, including hydroxide and sulfide precipitation [2,3].

Much research has been developed on the use of sorbents or biosorbents for heavy metals removal [4]. Generally, adsorption and ion exchange processes for metal ions removal were inhibited in aqueous solution containing chelating agents [5]. Application of the Fenton reaction followed by hydroxide precipitation in removing heavy metals from Ni-EDTA wastewater was investigated by Fu et al. [6]. Their results indicated that this process was effective at an optimized pH and H<sub>2</sub>O<sub>2</sub> dosage. Generally, the sludge was produced and needed to be disposed. Photocatalytic oxidation has been largely investigated and has shown promising results in oxidizing metal-EDTA complexes [7–10]. Particularly, photocatalytic

oxidation of the Ni-EDTA complex was performed in a semi-batch reactor equipped with four UV lamps by Salama and Berk [11]. In this process, the separation and recovery of TiO<sub>2</sub> particles were needed [12].

Electrochemical processes are usually used for the recovery of dissolved metal ions from industrial effluent streams [13,14]. Destruction of cyanide or EDTA at the anode and the recovery of heavy metals at the cathode were largely investigated [15,16]. In the case of Ni-EDTA, electrochemical oxidation of nickel-EDTA complex on a platinum electrode was reported [17]. An anodic electrodeposition procedure of nickel hydroxide and oxyhydroxide species using an alkaline bath containing Ni<sup>2+</sup> and EDTA as a ligand compound is described [18]. Besides, the literature related to nickel electrowinning was largely reported [19,20]. Electrodeposition of nickel ions from acidic solution in a cylindrical spouted electrochemical reactor was also reported [21]. Generally, anodic oxidation of organic complexes was characterized by a relatively low current efficiency.

The photoelectrocatalytic (PEC) process takes advantage of the photocatalysis by applying a biased voltage across a photo-electrode, which has been investigated in the degradation of organic contaminants [22–24], inactivation of bacteria [25,26]. However, little or no mention on the simultaneous recovery of metal ions at the cathode with oxidation of pollutants at the anode

\* Corresponding author at: P.O. Box 2871, 18 Shuangqing Road, Haidian District, Beijing 100085, PR China. Tel.: +86 010 62849151; fax: +86 010 62849160.

E-mail address: [jhqu@rcees.ac.cn](mailto:jhqu@rcees.ac.cn) (J. Qu).

was made in the earlier PEC process. In the current work, application of the PEC process in the destruction of Ni-EDTA at the anode and recovery of liberated nickel ions was examined. Effects of current density, pH value, and initial concentration of Ni-EDTA on the decomplexation of Ni-EDTA and recovery of nickel ions are investigated in details. Degradation intermediates at various pH conditions were identified and a degradation pathway of Ni-EDTA was proposed.

## 2. Experimental

### 2.1. Chemicals

Nickel(II) perchlorate hexahydrate ( $\text{Ni}(\text{ClO}_4)_2 \cdot 6\text{H}_2\text{O}$ ) and EDTA disodium salt were purchased from Beijing Yili Company and Sinopharm Chemical Reagent Co., Ltd., respectively. Nickel-EDTA solution was prepared by mixing equal molar ratio of  $\text{Ni}(\text{ClO}_4)_2 \cdot 6\text{H}_2\text{O}$  and  $\text{Na}_2\text{EDTA}$ . 10 mM  $\text{HClO}_4$  or 10 mM NaOH was used to adjust pH of the Ni-EDTA solutions. Similarly, Ni-iminodiacetic acid (Ni-IDA), Ni-nitrilotriacetic acid (Ni-NTA), and Ni-ethylendiamine diacetate (Ni-EDDA) were prepared with the equal molar ratio. Other reagents of analytical grade were obtained from Beijing Chemical Company (PR China) and were used as received. Deionized water was used for the preparation and dilution of all solutions.

### 2.2. Setup and experiment

The  $\text{TiO}_2/\text{Ti}$  film electrode ( $100\text{ mm} \times 60\text{ mm} \times 0.5\text{ mm}$ ) was used as an anode with an active area of  $60\text{ cm}^2$ .  $\text{TiO}_2$  film was deposited onto Ti plate via a dip-coating method [27]. The stainless steel with the same active area was used as cathode. The power was provided by a DC power supply source DH1718E-4 (Dahua Instrument Corporation of Beijing). Experiments of photocatalysis, electrolysis, and the PEC process were performed in a 500 mL, a single compartment cell with a 3.5 cm-diameter quartz tube placed in the center and used as the UV bulb housing. UV irradiation was provided by a 5 W-UV lamp (254 nm) and the light intensity at the center of the compartment was  $1.5\text{ mW/cm}^2$  measured with a UV radiometer (Light and Electric instruments Factory of Beijing Normal University). 10 mM  $\text{NaClO}_4$  was used as electrolyte solution. The reaction solution (450 mL) was put in the reaction cell and 5 mL sample was taken at a given time for the analysis.

### 2.3. Analytical procedures

Concentration of Ni-EDTA was determined using a high performance liquid chromatography (HPLC) (1260, Agilent Technology) equipped with a C-18 column (Agilent Technology) and two detectors connected in series, namely a diode array detector (Waters 996) and a fluorescence detector (Waters 474). The mobile phase consisted of 75:25 solvent:acetonitrile at a flow rate of 1 mL/min and a column temperature of 25 °C. The solvent was composed of 20 mM ammonium phosphate buffer to pH 2.0. The generated intermediates were measured using an ion chromatography (ICS-2000, Dionex, U.S.A.) with a conductivity detector. A capillary electrophoresis (P/ACETM MDQ) was used to identify the intermediates. An uncoated fused silica capillary, 50 cm in length (to the detector) and 75 µm in diameter, was used with UV detection at 185 nm. The carrier electrolyte was 50 mM phosphate and 0.5 mM tetradecyltrimethylammonium bromide (TTAB) (pH 6.8). Concentrations of  $\text{Ni}^{2+}$  ions were measured using a 710 series inductively coupled plasma optical emission spectrometer (ICP-OES, Agilent Technology, U.S.A.). Total organic carbon (TOC) was measured using a Shimadzu TOC analyzer (TOC-VCPH, Shimadzu, Japan). The

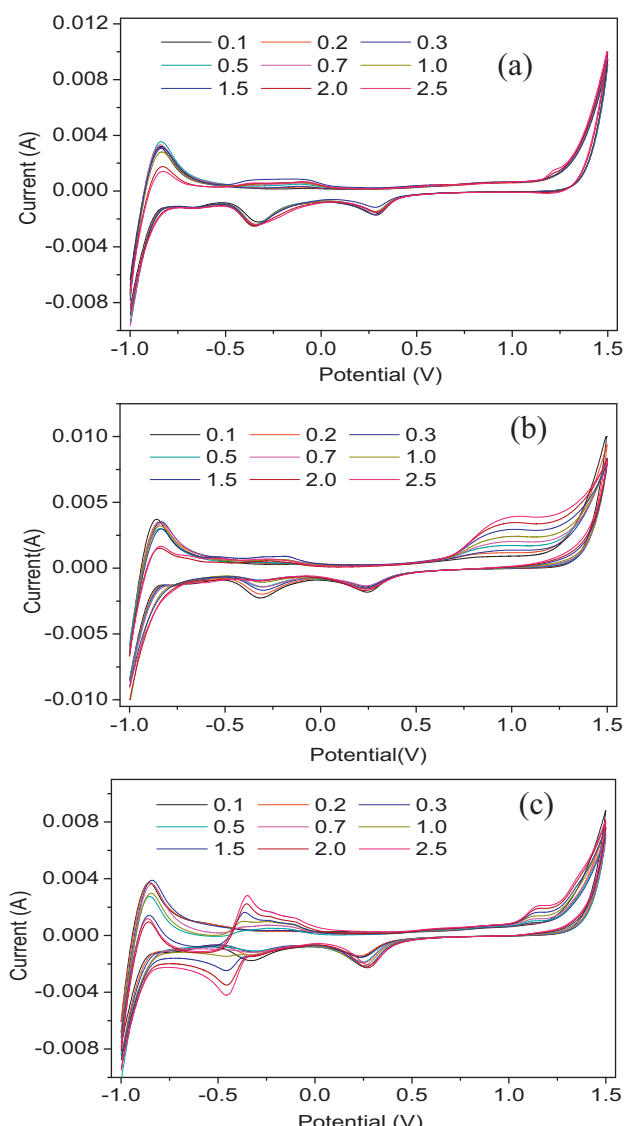


**Fig. 1.** Cyclic voltammery curves of  $\text{Ni}^{2+}$  (a), EDTA (b), Ni-EDTA (c) with various concentrations ( $\mu\text{M}$ ) at the  $\text{TiO}_2$  film electrode in 0.5 M  $\text{NaClO}_4$  solution.

chemical equilibrium model for the calculation of Ni-EDTA at various pH values is calculated via Visual MINTEQ ver.3.0.

The energy dispersive X-ray spectroscopy of the cathode was obtained using a JSM-7401 field emission system (JEOL, Japan). X-ray photoelectron spectra (XPS) were used to analyze the surface variation of the electrode using a PHI Quantera SXM (PHI-5300/ESCA, ULVAC-PHI, INC). The cyclic voltammery (CV) was conducted in a single-compartment, three electrode cell on a CHI 660b instrument (CH Instrument Co.). The electrolyte volume was 60 mL. The  $\text{TiO}_2$  films deposited onto Ti sheet was used as the anode; a platinum wire was used as the counter electrode. And, saturated calomel electrode (Shanghai Leichi Instrument Factory) was employed as the reference electrode. 0.5 M  $\text{NaClO}_4$  solution was used as electrolyte solution.

## 3. Results and discussion

### 3.1. Cyclic voltammery analysis

The electrochemical behaviors of  $\text{Ni}^{2+}$ , EDTA, and Ni-EDTA were investigated by CV at the prepared  $\text{TiO}_2/\text{Ti}$  electrode in solution

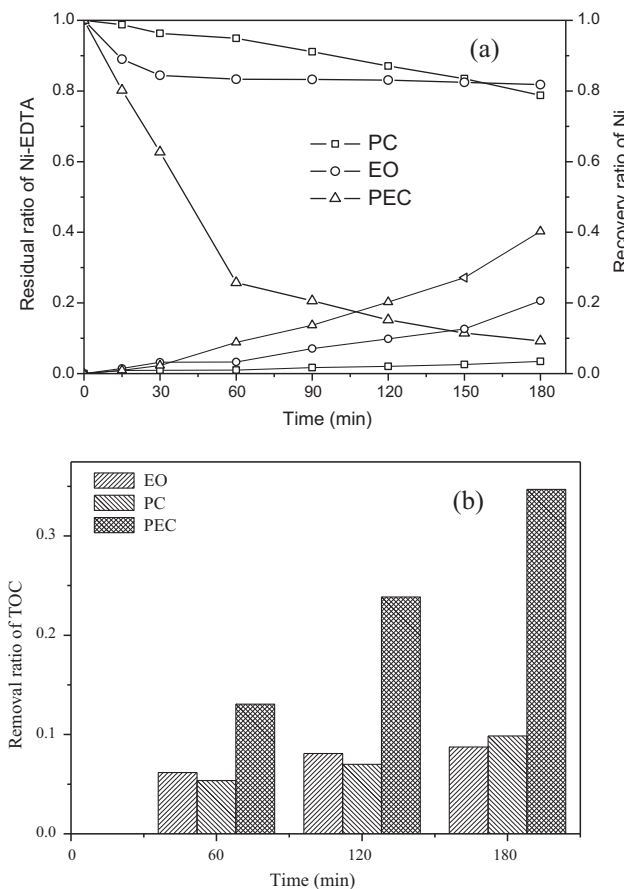


**Fig. 2.** (a) Removal of Ni-EDTA and recovery of nickel ions in the photocatalytic (PC), electro-oxidation (EO), and photoelectrocatalysis (PEC) processes; (b) the removal efficiency of total organic carbon in PC, EO, and PEC processes with the reaction time ( $[Ni\text{-EDTA}]_0 = 0.05 \text{ mM}$ , pH 6.6, current density =  $0.3 \text{ mA/cm}^2$ ).

with  $0.5 \text{ M NaClO}_4$  at a potential range from  $-1.00 \text{ V}$  to  $1.50 \text{ V}$  vs. SCE. All CV experiments were completed in the same conditions. It is seen from Fig. 1(a) that  $\text{Ni}^{2+}$  ions have no oxidation peaks in the potential from 0 to  $1.20 \text{ V}$ ; the oxidation peak potential of EDTA appears at about  $0.85 \text{ V}$  and peak intensity increases with the EDTA concentration (Fig. 1(b)); By contrast, the oxidation peak of Ni-EDTA is shifted to be  $1.20 \text{ V}$  (Fig. 1(c)). The shift from  $0.85$  to  $1.20 \text{ V}$  indicates the higher stability of Ni-EDTA than EDTA. And, the current intensity of Ni-EDTA is weaker than that for EDTA at a same concentration, which furthermore confirms that Ni-EDTA is more stable and difficult to be oxidized.

### 3.2. Efficiency of photoelectrocatalysis in relation to photocatalysis and electro-oxidation process

It can be seen from Fig. 2(a) that Ni-EDTA is efficiently removed in the PEC process in comparison with individual photocatalytic (PC) and electro-oxidation (EO) process. At 60 min, removal percentages of Ni-EDTA are determined to be 75%, 12%, and 5%, respectively. When the reaction time is extended to be 180 min, the removal percentages of Ni-EDTA in the PC and EO processes are 21% and 18%, respectively. By contrast, nearly 90% Ni-EDTA is removed in the PEC process. The variation of HPLC spectra with reaction time in PC, EO, and PEC processes as a function of reaction time was given in Fig. SM-1. It can be seen that the peak of Ni-EDTA is largely decreased in the PEC process, which confirms the decomposition of Ni-EDTA in the PEC process. The variation of TOC in the PC, EO, and PEC processes with the reaction time is presented

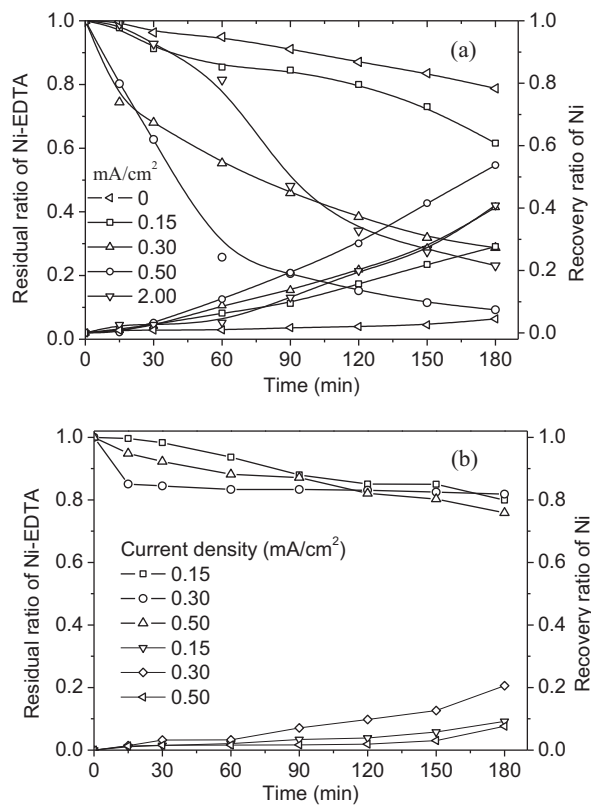


**Fig. 3.** Variation of Ni-EDTA concentration during (a) photoelectrocatalytic process and (b) electro-oxidation processes as a function of current density. ( $[Ni\text{-EDTA}]_0 = 0.05 \text{ mM}$ ; pH 6.6).

in Fig. 2(b). It can be seen that the TOC removal efficiency in the PEC process is significantly larger than that in the individual PC and EO process. These results indicate that the decomplexation intermediates of Ni-EDTA are mineralized to some extent in the PEC process. The organic acids with small molecular weight may contribute to the residual TOC. Identification of the intermediates will be given subsequently.

The recovery percentage of nickel ions was calculated as follows:  $(\text{initial concentration of total nickel} - \text{residual concentration of nickel})/\text{initial concentration of nickel}$ . Based on the data of Fig. 2(a), it is determined to be 45%, 21%, and 5% in the PEC, EO, and PC process, respectively. It can be concluded that the efficient destruction of Ni-EDTA complex is responsible for the high recovery percentage of nickel ions in the PEC process. The analysis of the nickel ions onto the cathode will be discussed subsequently.

### 3.3. Influencing factors

Effect of current density on the destruction of Ni-EDTA and nickel recovery in the EO and PEC process was investigated with  $0.05 \text{ mM Ni-EDTA}$  at pH 6.6. The cell voltage was allowed to vary so that the experiments were performed at a constant current density. It can be seen from Fig. 3(a) and (b) that the removal rates of Ni-EDTA in the PEC and EO process increase with the current density. The destruction efficiencies of Ni-EDTA and recovery percentage of nickel ions are significantly lower than that in the PEC process. It is known that application of a low current density increases the photocatalytic degradation rate by promoting the separation of photo-generated electron and hole. With the increase of applied current density, the direct EO and PC processes occur simultaneously and contribute to the synergistic removal of Ni-EDTA and recovery of nickel ions; when the applied bias potential is

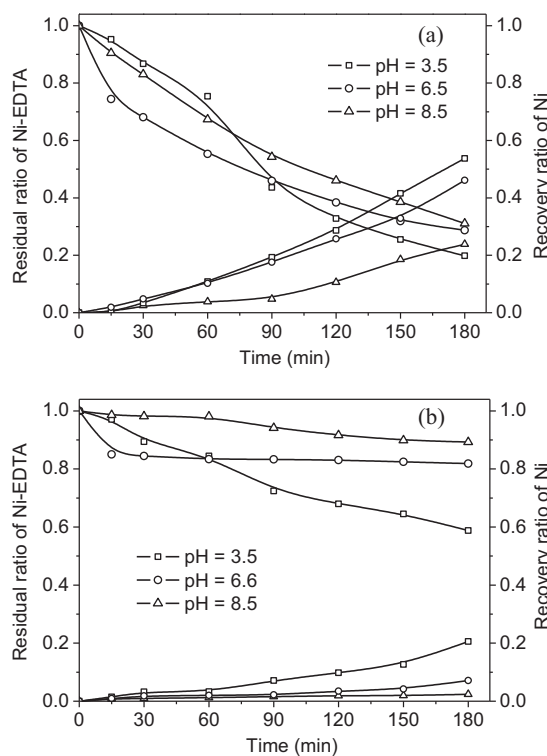


**Fig. 4.** Variation of initial solution pH on the destruction of Ni-EDTA and nickel recovery during the photoelectrocatalytic process (a) and electro-oxidation process (b) ( $[Ni\text{-EDTA}]_0 = 0.05 \text{ mM}$ ; current density =  $0.3 \text{ mA}/\text{cm}^2$ ).

furthermore increased, indirect EO and PC processes of Ni-EDTA occur, which contributes to the high destruction rate of Ni-EDTA. The similar trend has been reported in our previous work for the PEC degradation of anti-inflammatory pharmaceuticals [28].

Degradation of Ni-EDTA and recovery of  $\text{Ni}^{2+}$  ions at various pH values in the PEC and EO process was performed with a constant current density. As shown in Fig. 4(a) and (b), the degradation of Ni-EDTA favors at acid conditions in the PEC and EO process. It is also observed that the recovery percentage of the nickel ions increases with the decrease of pH value in the EO and PEC processes. As seen from Fig. SM-2, Ni-EDTA is the only component of nickel complexed with EDTA when solution pH is between 5.0 and 11.0; and  $\text{Ni-EDTA}^{2-}$  is the most stable component of all species of nickel complexed with EDTA. Therefore,  $\text{Ni-EDTA}^{2-}$  could exist stably at a large pH range. When the solution pH is at 3.5,  $\text{Ni-EDTA}^{2-}$  and  $\text{NiHEDTA}^-$  is half of all Ni-EDTA, respectively. Maybe, the oxidation reaction of generated  $\cdot\text{OH}$  in the PEC process with  $\text{NiHEDTA}^-$  is better than with  $\text{Ni-EDTA}^{2-}$ . With respect to the electrodeposition of  $\text{Ni}^{2+}$  ions liberated from the decomplexation of Ni-EDTA,  $\text{Ni}^{2+}$  ions are readily released into the solution and adsorbed onto the cathode at low pH, which becomes adsorbed onto the  $\text{TiO}_2$  film surface at neutral pH. As a result, higher nickel ions recovery was obtained at lower pH. Meantime, at high pH condition, formation of insoluble hydroxides at the cathode surfaces becomes easy [20,29]. Therefore, the deposition of nickel ions on the cathode surface will be inhibited in the PEC process at high pH condition. In addition, high destruction rate of Ni-EDTA at acid condition can also partially be attributed to the increased potentials of valence band hole at low pH values in the  $\text{TiO}_2$  photocatalytic process [30].

Effect of initial Ni-EDTA concentrations on the destruction of Ni-EDTA and recovery of  $\text{Ni}^{2+}$  ions was performed with the constant current density of  $0.3 \text{ mA}/\text{cm}^2$ . As shown in Fig. 5, the removal of Ni-EDTA and recovery of  $\text{Ni}^{2+}$  ions is the largest at the initial Ni-EDTA concentration of  $0.050 \text{ mM}$  in comparison with  $0.025$  and

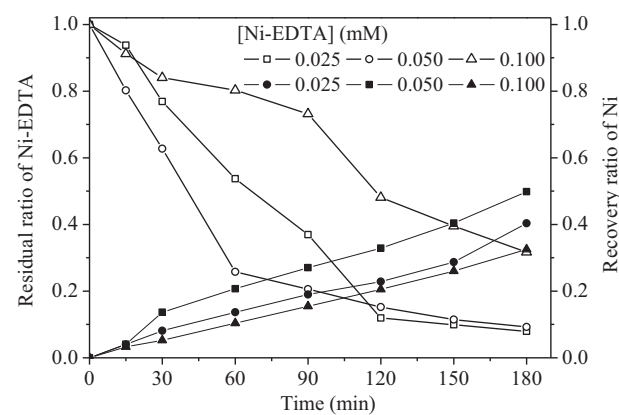


**Fig. 5.** Effect of initial Ni-EDTA concentrations on the destruction of Ni-EDTA and recovery of nickel in the photoelectrocatalytic process (current density =  $0.3 \text{ mA}/\text{cm}^2$ ; pH 6.6).

$0.100 \text{ mM}$ . As expected, increase of the Ni-EDTA complex concentration increases solution conductivity and the driving force for mass transfer, and thus facilitates the PEC reaction of Ni-EDTA and metal deposition onto the cathode. In addition, this would reduce the occurrence of side reactions and thus increase nickel recovery and current density [31]. When the concentration of Ni-EDTA is increased to a certain value, the amount of Ni-EDTA reacting with the generated  $\cdot\text{OH}$  radicals at the anode is enough, excess Ni-EDTA will decrease the rate of decomplexation of Ni-EDTA by trapping the absorption sites at the electrode [23,32]. As a result, the Ni-EDTA destruction and nickel recovery is inhibited.

In the photocatalytic system,  $\text{HCO}_3^-/\text{CO}_3^{2-}$  pair could scavenge hydroxyl radicals yielding carbonate radical anions. Therefore, rates of the possible competitive reactions between hydroxyl

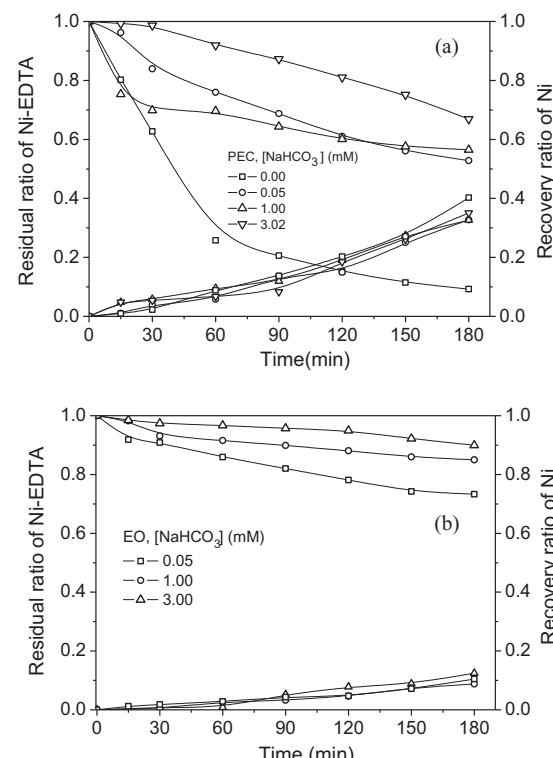


**Fig. 6.** The effect of  $\text{HCO}_3^-$  on the destruction of Ni-EDTA and recovery of  $\text{Ni}^{2+}$  ions in the photoelectrocatalytic process (a) and electro-oxidation process (b) ( $[Ni\text{-EDTA}]_0 = 0.05 \text{ mM}$ ; current density =  $0.3 \text{ mA}/\text{cm}^2$ ).

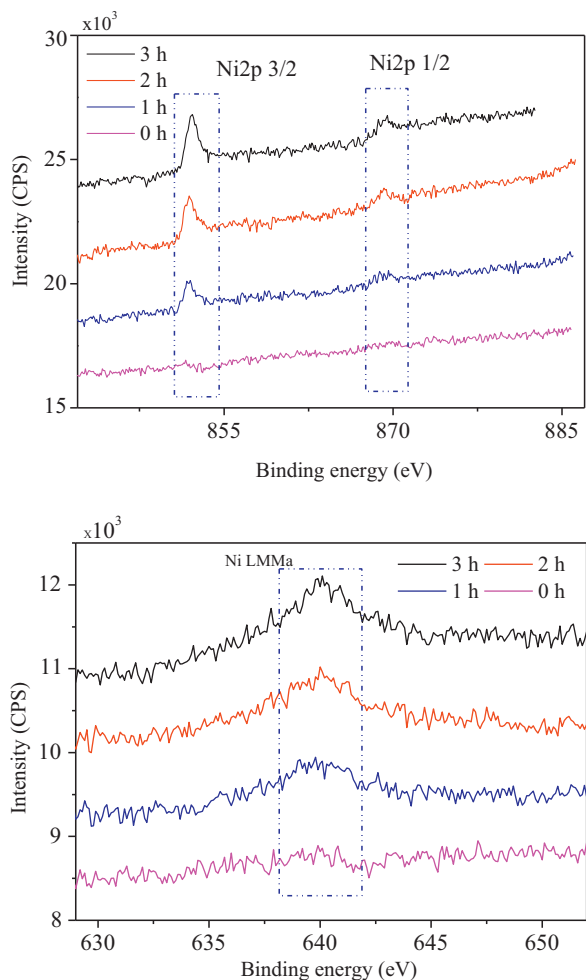


**Fig. 7.** X-ray photoelectron spectra analysis of the surface variations of the cathode in the photoelectrocatalytic process with the reaction time ( $[Ni\text{-EDTA}]_0 = 0.05 \text{ mM}$ , pH 6.6, current density =  $0.3 \text{ mA/cm}^2$ ).

radicals and targeted substances decreased gradually with an increase in the concentration of carbonate species [33]. Herein, effect of  $\text{HCO}_3^-$  ions on the destruction of Ni-EDTA and recovery of  $\text{Ni}^{2+}$  ions was investigated in the EO and PEC process. It can be seen from Fig. 6(a) that the destruction of Ni-EDTA and recovery of  $\text{Ni}^{2+}$  ions is inhibited in the presence of  $\text{NaHCO}_3$ . Similar trend is observed in the case of the EO process (Fig. 6(b)). The above results indicate that  $\cdot\text{OH}$  radicals are mainly responsible for the destruction of Ni-EDTA complex. It was noticed that the recovery of the  $\text{Ni}^{2+}$  ions was not affected by the concentration of  $\text{NaHCO}_3$ . In the current work, the recovery efficiency of the nickel ions was low even without the addition of  $\text{NaHCO}_3^-$ . And, the inhibition effect was also slight. Meantime, the precipitation between the liberated  $\text{Ni}^{2+}$  ions from Ni-EDTA and  $\text{HCO}_3^-$  occurred, which may decrease the recovery efficiency of the  $\text{Ni}^{2+}$  ions. The amount of  $\text{HCO}_3^-$  was enough to precipitate the  $\text{Ni}^{2+}$  ions even at the concentration of 0.05 mM.

### 3.4. Electrodeposition process of $\text{Ni}^{2+}$ ions at the cathode

The EDX analysis of the steel stainless cathode with the reaction evolution was performed. As shown in Fig. SM-3 and Table SM1, amount of nickel at the cathode increases with the evolution of reaction time, which confirms the nickel recovery by the electrodeposition process. X-ray photoelectron spectroscopy was used to probe the chemical nature and oxidation state of the

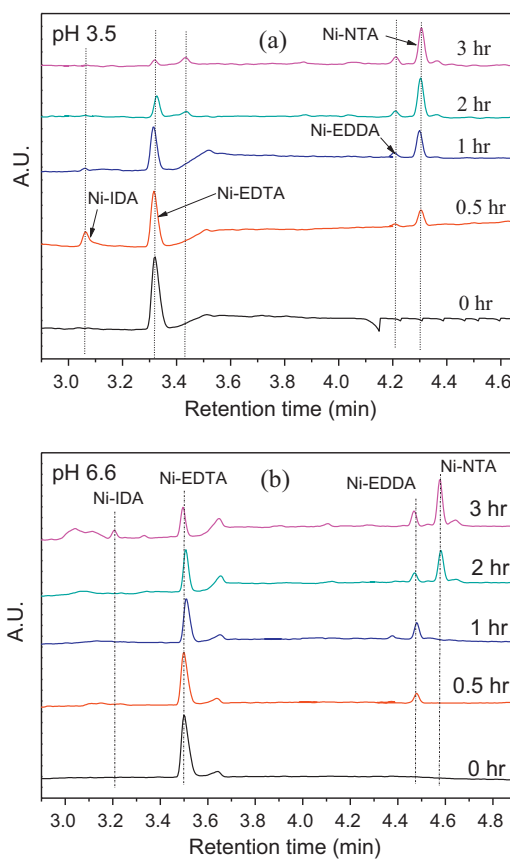


**Fig. 8.** Electropherograms of Ni-EDTA solution treated at various time in the PEC oxidation conditions: 50 mM phosphate buffer and 0.5 mM TTAB (pH 6.8), 195 nm, 20 kV, 25 °C. AU = absorbance units. (a) at pH 3.5; (b) at pH 6.6 ( $[Ni\text{-EDTA}]_0 = 0.05 \text{ mM}$ , current density =  $0.3 \text{ mA/cm}^2$ ).

electrodeposited nickel film on the cathode. Throughout this study, the  $\text{Ni}2\text{P}_{3/2}$ , O1s and C1s regions were collected and analyzed for each specimen. As shown in Fig. 7, the peak of  $\text{Ni}2\text{P}_{3/2}$  appears at 852.0 eV, which increases with the time evolution. The peak at 853.0 eV is ascribed to the elemental Ni [34]. No trace of other nickel crystals is detected.

It has been reported that two one-electron metal reduction reactions take place in succession [35]. The presence of a highly stable  $\text{Ni(OH)}_2$  phase generated at the cathode may suppress the adsorption of reactive intermediates for nickel deposition. The overall deposition process is as follows (Eqs. (1)–(4)).



$\text{Ni(OH)}_2$  precipitation at the electrode could substantially lower the effective adsorption of reactive intermediate  $\text{Ni}(\text{OH})_{\text{ads}}$ . In the present study, the electrodeposition of liberated nickel ions often does not proceed at high recovery efficiency. Because of this hydrogen evolution occurring at the cathode, the hydrogen ion is depleted near the cathode surface. When the supply of hydrogen ions is unable to meet the depletion rate, the cathode surface pH will rise and eventually lead to the formation of insoluble nickel hydroxide on the cathode surface, which will decrease the efficiency of the nickel recovery.

**Table 1**

Identified intermediates of Ni-EDTA destruction by the photoelectrocatalytic process.

	Retention time (min)	Molecular name	Molecular formula	Structure formula
(a)	7.3	Glycine <sup>a,b</sup>	C <sub>2</sub> H <sub>5</sub> O <sub>2</sub> N	
(b)	9.8	Maleic acid <sup>a,b</sup>	C <sub>4</sub> H <sub>4</sub> O <sub>4</sub>	
(c)	11.5	Glycolic acid <sup>a,b</sup>	C <sub>2</sub> H <sub>4</sub> O <sub>3</sub>	
(d)	13.2	Formic acid <sup>a</sup>	CH <sub>2</sub> O <sub>2</sub>	
(e)	14.3	Acetic acid <sup>a,b</sup>	C <sub>2</sub> H <sub>4</sub> O <sub>2</sub>	
(f)	16.7	Oxalic acid <sup>a</sup>	C <sub>2</sub> H <sub>2</sub> O <sub>4</sub>	
(g)	18.3	Oxamic acid <sup>a,b</sup>	C <sub>2</sub> H <sub>3</sub> O <sub>3</sub> N	

<sup>a</sup> pH 3.5.<sup>b</sup> pH 6.6.

### 3.5. Identification of reaction intermediates and a proposed decomplexation pathway

In the PEC process, the generated intermediates at pH 3.5 and 6.6 were identified by the EC and HPLC analysis, respectively. It can be seen from Fig. 8(a) that concentration of Ni-EDTA decreases with the increase of Ni-NTA in the reaction process at pH 3.5. Meantime, Ni-IDA is detected at 0.5 h and Ni-EDDA is also observed for the samples at 1, 2, and 3 h. A slight difference is observed from Fig. 8(b). At pH 6.6. Ni-NTA and Ni-IDA appears at 2 and 3 h, respectively.

As shown in Table 1 and Fig. 9(a), intermediates including glycine, maleic acid, glycolic acid, formic acid, acetic acid, oxalic acid, and oxamic acid are identified at pH 3.5. By contrast, formic acid and oxalic acid are not identified at pH 6.6 (Fig. 9(c)). The concentration variation of these intermediates with the reaction time at pH 3.5 and 6.6 is presented in Fig. 9(b) and (d), respectively. At pH 3.5, concentration of glycine and oxamic acid increases with the reaction time up to 150 min. The concentration of acetic acid, formic acid, and oxalic acid is relatively low. An obvious difference of the concentration variations of glycine, maleic acid, glycolic acid, acetic acid, and oxalic acid is observed at pH 6.6. Concentration of

oxamic acid increases up to 200 mg/L at 180 min. By contrast, the concentration of glycine, maleic acid, glycolic acid, and acetic acid are less than 100 mg/L.

Meantime, NH<sub>4</sub><sup>+</sup> and NO<sub>3</sub><sup>-</sup> are also identified in the PEC process. As shown in Fig. SM-4, the amount of generated NH<sub>4</sub><sup>+</sup> and NO<sub>3</sub><sup>-</sup> is slight at the initial 90 min under all the conditions. After that, the amount of NH<sub>4</sub><sup>+</sup> and NO<sub>3</sub><sup>-</sup> are obviously increased. In the case of NH<sub>4</sub><sup>+</sup>, the generated amount at pH 6.6 is larger than that at pH 3.5 and 8.5. The generated amount of NO<sub>3</sub><sup>-</sup> ions increases with the initial solution pH, which favors at basic condition.

It has been proposed that the initial oxidation step occurred at the acetate group in the electrochemical oxidation of free EDTA on a Pt electrode at acid and alkaline solutions [36,37]. It was also recognized that the homogeneous photocatalytic reaction of EDTA occurred through its amine group at neutral pH [8,9] and its carboxylic group complexed into the TiO<sub>2</sub> surface at acidic pH [7]. As shown in Fig. 8, the peak intensity of Ni-NTA was obviously higher than that of Ni-EDDA and Ni-IDA. Thus, it was concluded that Ni-NTA was identified as main intermediates. Therefore, it is concluded that the decomplexation of Ni-EDTA is mainly through

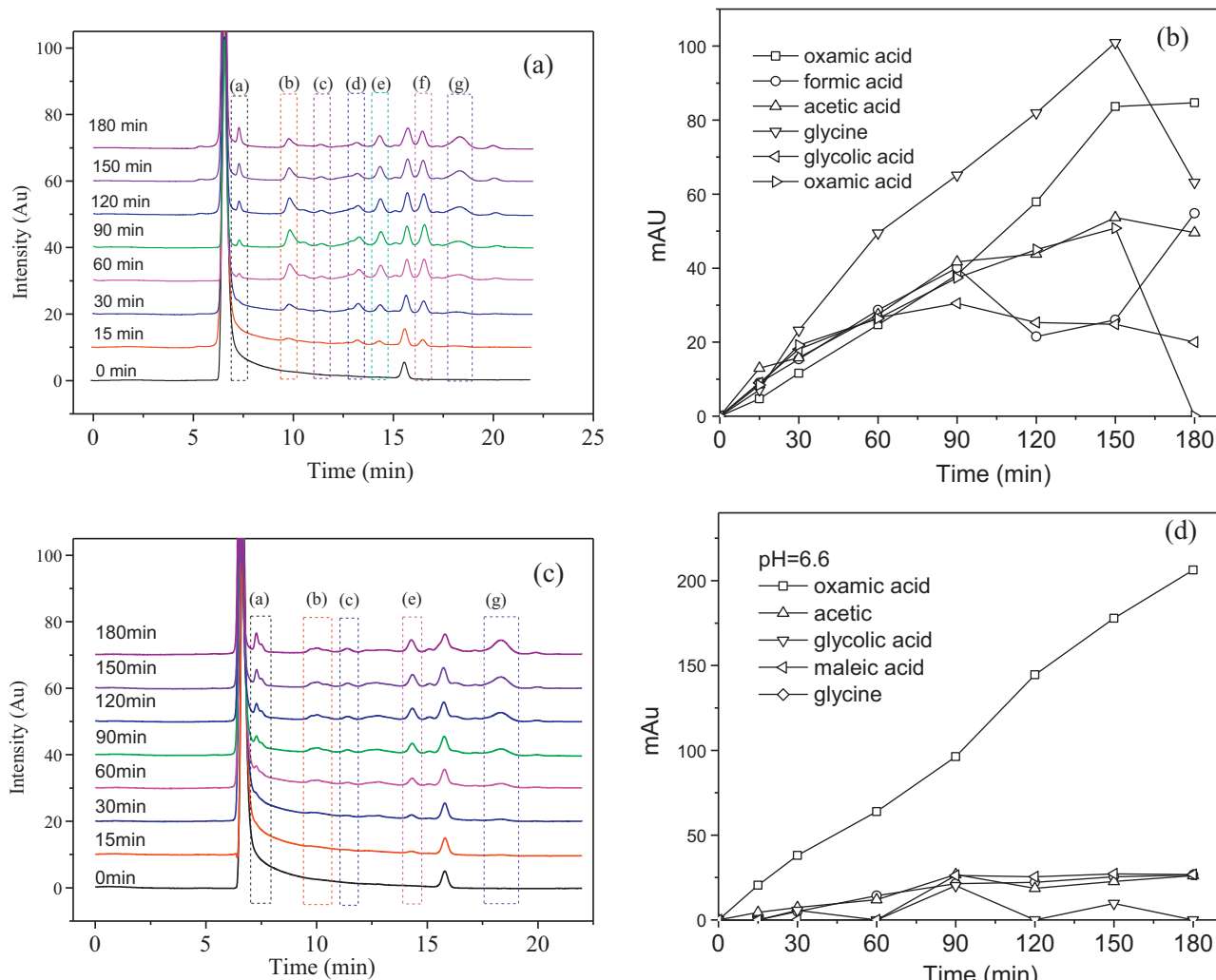


**Fig. 9.** Generated intermediates and their concentration variations with the reaction time in the photoelectrocatalytic process at pH 3.5 ((a), (b)) and pH 6.6 ((c), (d)) ( $[Ni\text{-EDTA}]_0 = 0.05 \text{ mM}$ ; current density =  $0.5 \text{ mA/cm}^2$ ).

the cleavage of amine group at Ni-EDTA groups, leading to the generation of Ni-NTA and Ni-IDDA. Ni-EDDA is generated via the removal of acetic group from Ni-EDTA. All above intermediates are furthermore decomposed into the small molecular acids and inorganic ions including  $\text{NH}_4^+$  and  $\text{NO}_3^-$ .

#### 4. Conclusions

The results obtained in the current work exhibit that the PEC system can be used to destroy Ni-EDTA complex with simultaneous recovery of nickel. And, nearly 40% of EDTA was mineralized. The removal of Ni-EDTA and recovery of nickel increased with the current density and favored at acid conditions. The presence of  $\text{HCO}_3^-$  ions inhibited the removal of Ni-EDTA and the recovery of nickel, which indicated the important role of  $\cdot\text{OH}$  radicals in the decomplexation of Ni-EDTA. Intermediates mainly including Ni-NTA, oxamic acid, formic acid, and acetic acid are identified; Nitrogen accumulates as  $\text{NH}_4^+$  and  $\text{NO}_3^-$ . It was concluded that the decomplexation of Ni-EDTA was mainly through the cleavage of amine group at Ni-EDTA with a slight removal of acetic group from Ni-EDTA. In further studies, we will focus on the process optimization and cost-efficiency evaluation of the proposed remediation method to broaden the practicality of the PEC processes.

#### Acknowledgments

This work was supported by National Natural Science Foundation of China (Nos. 51222802, 51221892).

#### Appendix A. Supplementary data

Supplementary data associated with this article can be found, in the online version, at <http://dx.doi.org/10.1016/j.apcatb.2013.07.038>.

#### References

- [1] M.E.T. Sillanpää, Biogeochemistry of Chelating Agents 910 (2005) 226–233.
- [2] O. Tünay, I. Kabdasli, R. Tasli, Water Science and Technology 29 (1994) 265–274.
- [3] C. Durante, M. Cuscov, A.A. Isse, A. Gennaro, Water Research 45 (2011) 2122–2130.
- [4] N. Akhtar, J. Iqbal, M. Iqbal, Journal of Hazardous Materials 108 (2004) 85–94.
- [5] F.C. Wu, R.L. Tseng, R.S. Juang, Industrial and Engineering Chemistry Research 38 (1999) 270–275.
- [6] F.L. Fu, B. Tang, W. Wang, J.Y. Liu, Environmental Chemistry Letters 8 (2010) 317–322.
- [7] D.N. Furlong, D. Wells, W.H.F. Saase, Australian Journal of Chemistry 39 (1986) 757–769.
- [8] J.K. Yang, A.P. Davis, Environmental Science & Technology 34 (2000) 3796–3801.
- [9] J.K. Yang, A.P. Davis, Environmental Science & Technology 34 (2000) 3789–3795.

[10] K. Kabra, R. Chaudhary, R.L. Sawhney, Industrial and Engineering Chemistry Research 43 (2004) 7683–7696.

[11] P. Salama, D. Berk, Industrial and Engineering Chemistry Research 44 (2005) 7071–7077.

[12] M.N. Chong, B. Jin, C.W.K. Chow, C. Saint, Water Research 44 (2010) 2997–3027.

[13] G.H. Chen, Separation and Purification Technology 38 (2004) 11–41.

[14] D. Voglar, D. Lestan, Water Research 46 (2012) 1999–2008.

[15] S.C. Cheng, M.T. Gattrell, B.M. Guena, Electrochimica Acta 47 (2002) 3245–3256.

[16] N.S. Bhadrinarayana, B.C. Ahmed, N. Anantharaman, Industrial and Engineering Chemistry Research 46 (2007) 6417–6424.

[17] E. Fuchs, G. Ginsburg, J. Lati, Journal of Electrochemical Interfaces Electrochemistry 73 (1976) 83–90.

[18] I.G. Casella, R. Spera, Journal of Electroanalytical Chemistry 578 (2005) 55–62.

[19] I. Epelboin, M. Joussetin, R. Wiart, Journal of Electrochemical Interfaces Electrochemistry 119 (1981) 61–71.

[20] C.Q. Cui, J.Y. Lee, Electrochimica Acta 40 (1995) 1653–1662.

[21] P. Grimshaw, J.M. Calo, P.A. Shirvaniyan, G. Hradil, Industrial and Engineering Chemistry Research 50 (2011) 9525–9531.

[22] H.T. Yu, S. Chen, X. Quan, H.M. Zhao, Y.Z. Zhang, Applied Catalysis B: Environmental 90 (2009) 242–248.

[23] Z. Frontistis, V.M. Daskalaki, A. Katsaounis, I. Poulios, D. Mantzavinos, Water Research 45 (2011) 2996–3004.

[24] K. Li, Y. He, Y.L. Xu, Y.L. Wang, J.P. Jia, Environmental Science and Technology 45 (2011) 7401–7407.

[25] G.Y. Li, X.L. Liu, H.M. Zhang, T.C. An, S.Q. Zhang, A.R. Carroll, Journal of Catalysis 277 (2011) 88–94.

[26] Y. Hou, X.Y. Li, Q.D. Zhao, G.H. Chen, C.L. Raston, Environmental Science and Technology 46 (2012) 4042–4050.

[27] J. Shang, W. Li, Y.F. Zhu, Journal of Molecular Catalysis A: Chemical 202 (2003) 187–195.

[28] X. Zhao, J.H. Qu, H.J. Liu, Z.M. Qiang, R.P. Liu, C.Z. Hu, Applied Catalysis B: Environmental 91 (2009) 539–545.

[29] J. Ji, W.C. Cooper, D.B. Dreisinger, E. Peters, Journal of Applied Electrochemistry 25 (1995) 642–650.

[30] T.H. Madden, A.K. Datye, M. Fulton, Environmental Science and Technology 31 (1997) 3475–3481.

[31] R.-S. Juang, S.-W. Wang, Water Research 34 (2000) 3179–3185.

[32] M.H. Abdel-Aziz, I. Nirdosh, G.H. Sedahmed, Industrial and Engineering Chemistry Research 51 (2012) 11636–11642.

[33] H. Selcuk, Water Research 44 (2010) 3966–3972.

[34] H. Li, H.X. Li, W.L. Dai, W.J. Wang, Z.G. Fang, J.F. Deng, Applied Surface Science 152 (1999) 25–34.

[35] W.G. Proud, C. Müller, Electrochimica Acta 38 (1993) 405–413.

[36] J.W. Johnson, H.W. Jiang, S.B. Hanna, W.J. James, Journal of the Electrochemical Society 119 (1972) 574–579.

[37] S.N.R. Pakalapati, B.N. Popov, R.E. White, Journal of the Electrochemical Society 143 (1996) 574–579.